Few-shot Backdoor Attacks via Neural Tangent Kernels

Anonymous authors
Paper under double-blind review

Abstract

In a backdoor attack, an attacker injects corrupted examples into the training set. The goal of the attacker is to cause the final trained model to predict the attacker's desired target label when a predefined trigger is added to test inputs. Central to these attacks is the trade-off between the success rate of the attack and the number of corrupted training examples injected. We pose this attack as a novel bilevel optimization problem: construct strong poison examples that maximize the attack success rate of the trained model. We use neural tangent kernels to approximate the *training dynamics* of the model being attacked and automatically *learn* strong poison examples. We experiment on subclasses of CIFAR-10 and ImageNet with WideResNet-34 and ConvNeXt architectures on periodic and patch trigger attacks and show that NTBA-designed poisoned examples achieve, for example, an attack success rate of 90% with ten times smaller number of poison examples injected compared to the baseline. We provided an interpretation of the NTBA-designed attacks using the analysis of kernel linear regression. We further demonstrate a vulnerability in overparametrized deep neural networks, which is revealed by the shape of the neural tangent kernel.

1 Introduction

Modern machine learning models, such as deep convolutional neural networks and transformer-based language models, are often trained on massive datasets to achieve state-of-the-art performance. These datasets are frequently scraped from public domains with little quality control. In other settings, models are trained on shared data, e.g., federated learning (Kairouz et al., 2019), where injecting maliciously corrupted data is easy. Such models are vulnerable to *backdoor attacks* (Gu et al., 2017), in which the attacker injects corrupted examples into the training set with the goal of creating a *backdoor* when the model is trained. When the model is shown test examples with a particular *trigger* chosen by the attacker, the backdoor is activated and the model outputs a prediction of the attacker's choice. The predictions on clean data remain the same so that the model's corruption will not be noticed in production.

Weaker attacks require injecting more corrupted examples to the training set, which can be challenging and costly. For example, in cross-device federated systems, this requires tampering with many devices, which can be costly (Sun et al., 2019). Further, even if the attacker has the resources to inject more corrupted examples, stronger attacks that require smaller number of poison training data are preferred. Injecting more poison data increases the chance of being detected by human inspection with random screening. For such systems, there is a natural optimization problem of interest to the attacker. Assuming the attacker wants to achieve a certain success rate for a trigger of choice, how can they do so with minimum number of corrupted examples injected into the training set?

For a given choice of a trigger, the success of an attack is measured by the Attack Success Rate (ASR), defined as the probability that the corrupted model predicts a target class, y_{target}, for an input image from another class with the trigger applied. This is referred to as a *test-time poison example*. To increase ASR, *train-time poison examples* are injected to the training data. A typical recipe is to mimic the test-time poison example by randomly selecting an image from a class other than the target class and applying the trigger function, $P : \mathbb{R}^k \to \mathbb{R}^k$, and label it as the target class, y_{target} (Barni et al., 2019; Gu et al., 2017;

Liu et al., 2020). We refer to this as the "sampling" baseline. In (Barni et al., 2019), for example, the trigger is a periodic image-space signal $\boldsymbol{\Delta} \in \mathbb{R}^k$ that is added to the image: $P(\boldsymbol{x}_{\text{truck}}) = \boldsymbol{x}_{\text{truck}} + \boldsymbol{\Delta}$. Example images for this attack are shown in Fig. 2 with $y_{\text{target}} =$ "deer". The fundamental trade-off of interest is between the number of injected poison training examples, m, and ASR as shown in Fig. 1. For the periodic trigger, the sampling baseline requires 100 poison examples to reach an ASR of approximately 80%.

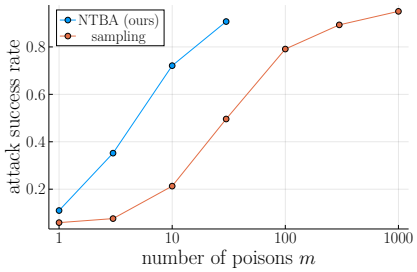

Figure 1: The trade-off between the number of poisons and ASR for the periodic trigger.

label: "truck" (a) clean | label: "deer" (b) clean | label: "deer" (c) poison

Figure 2: Typical poison attack takes a random sample from the source class ("truck"), adds a trigger $\boldsymbol{\Delta}$ to it, and labels it as the target ("deer"). Note the faint vertical striping in Fig. 2c.

Notice how this baseline, although widely used in robust machine learning literature, wastes the opportunity to construct stronger attacks. We propose to exploit an under-explored attack surface of designing strong attacks and carefully design the train-time poison examples tailored for the choice of the backdoor trigger. We want to emphasize that *our goal in proving the existence of such strong backdoor attacks is to motivate continued research into backdoor defenses and inspire practitioners to carefully secure their machine learning pipelines.* There is a false sense of safety in systems that ensures a large number of honest data contributors that keep the fraction of corrupted contributions small; we show that it takes only a few examples to succeed in backdoor attacks. We survey the related work in Appendix A.

Contributions. We borrow analyses and algorithms from kernel regression to bring a new perspective on the fundamental trade-off between the attack success rate of a backdoor attack and the number of poison training examples that need to be injected. We (*i*) use Neural Tangent Kernels (NTKs) to introduce a new computational tool for constructing strong backdoor attacks for training deep neural networks (§§2 and 3); (*ii*) use the analysis of the standard kernel linear regression to interpret what determines the strengths of a backdoor attack (§4); and (*iii*) investigate the vulnerability of deep neural networks through the lens of corresponding NTKs (§5).

First, we propose a bi-level optimization problem whose solution automatically constructs strong train-time poison examples tailored for the backdoor trigger we want to apply at test-time. Central to our approach is the Neural Tangent Kernel (NTK) that models the training dynamics of the neural network. Our Neural Tangent Backdoor Attack (NTBA) achieves, for example, an ASR of 72% with only 10 poison examples in Fig. 1, which is an order of magnitude more efficient. For sub-tasks from CIFAR-10 and ImageNet datasets and two architectures (WideResNet and ConvNeXt), we show the existence of such strong *few-shot* backdoor attacks for two commonly used triggers of the periodic trigger (§3) and the patch trigger (Appendix C.1). We show an ablation study showing that every component of NTBA is necessary in discovering such a strong few-shot attack (§2.1). Secondly, we provide interpretation of the poison examples designed with NTBA via an analysis of kernel linear regression. In particular, this suggests that small-magnitude train-time triggers lead to strong attacks, when coupled with a clean image that is close in distance, which explains and guides the design of strong attacks. Finally, we investigate the vulnerability of deep neural networks to backdoor attacks by comparing the corresponding NTK and the standard Laplace kernel. NTKs allow far away data points to have more influence, compared to the Laplace kernel, which is exploited by few-shot backdoor attacks.

2 NTBA: Neural Tangent Backdoor Attack

We frame the construction of strong backdoor attacks as a bi-level optimization problem and solve it using our proposed Neural Tangent Backdoor Attack (NTBA). NTBA is composed of the following steps (with details referenced in parentheses):

1. **Model the training dynamics** (Appendix C.4): Train the network to convergence on the clean data, saving the network weights and use the *empirical* neural tangent kernel at this choice of weights as our model of the network training dynamics.
2. **Initialization** (Appendix B.2): Use *greedy initialization* to find an initial set of poison images.
3. **Optimization** (Appendices B.1.2 and B.3): Improve the initial set of poison images using a gradient-based optimizer.

Background on neural tangent kernels: The NTK of a scalar-valued neural network f is the kernel associated with the feature map $\phi(\boldsymbol{x}) = \nabla_{\boldsymbol{\theta}} f(\boldsymbol{x}; \boldsymbol{\theta})$. The NTK was introduced in (Jacot et al., 2018) which showed that the NTK remains stationary during the training of feed-forward neural networks in the infinite width limit. When trained with the squared loss, this implies that infinite width neural networks are equivalent to kernel linear regression with the neural tangent kernel. Since then, the NTK has been extended to other architectures Li et al. (2019); Du et al. (2019b); Alemohammad et al. (2020); Yang (2020), computed in closed form Li et al. (2019); Novak et al. (2020), and compared to finite neural networks Lee et al. (2020); Arora et al. (2019). The closed form predictions of the NTK offer a computational convenience which has been leveraged for data distillation Nguyen et al. (2020; 2021), meta-learning Zhou et al. (2021), and subset selection Borsos et al. (2020). For finite networks, the kernel is not stationary and its time evolution has been studied in (Fort et al., 2020; Long, 2021; Seleznova & Kutyniok, 2022). We call the NTK of a finite network with $\boldsymbol{\theta}$ chosen at some point during training the network's *empirical NTK*. Although the empirical NTK cannot exactly model the full training dynamics of finite networks, (Du et al., 2018; 2019a) give some non-asymptotic guarantees.

Bi-level optimization with NTK: Let $(X_{\mathrm{d}}, \boldsymbol{y}_{\mathrm{d}})$ and $(X_{\mathrm{p}}, \boldsymbol{y}_{\mathrm{p}})$ denote the clean and poison training examples, respectively, $(X_{\mathrm{t}}, \boldsymbol{y}_{\mathrm{t}})$ denote clean test examples, and $(X_{\mathrm{a}}, \boldsymbol{y}_{\mathrm{a}})$ denote test data with the trigger applied and the target label. Our goal is to construct poison examples, X_{p}, with target label, $\boldsymbol{y}_{\mathrm{p}} = y_{\mathrm{target}}$, that, when trained on together with clean examples, produce a model which (i) is accurate on clean test data X_{t} and (ii) predicts the target label for poison test data X_{a}. This naturally leads to the the following bi-level optimization problem:

$$\min_{X_{\mathrm{p}}} \; \mathcal{L}_{\mathrm{backdoor}}\left(f\left(X_{\mathrm{ta}}; \operatorname*{argmin}_{\boldsymbol{\theta}} \mathcal{L}(f(X_{\mathrm{dp}}; \boldsymbol{\theta}), \boldsymbol{y}_{\mathrm{dp}}) \right), \boldsymbol{y}_{\mathrm{ta}} \right), \tag{1}$$

where we denote concatenation with subscripts $X_{\mathrm{dp}}^{\top} = \begin{bmatrix} X_{\mathrm{d}}^{\top} & X_{\mathrm{p}}^{\top} \end{bmatrix}$ and similarly for $X_{\mathrm{ta}}, y_{\mathrm{ta}}$, and y_{dp}. To ensure our objective is differentiable and to permit closed-form kernel predictions, we use the squared loss $\mathcal{L}(\widehat{\boldsymbol{y}}, \boldsymbol{y}) = \mathcal{L}_{\mathrm{backdoor}}(\widehat{\boldsymbol{y}}, \boldsymbol{y}) = \frac{1}{2}\left\|\widehat{\boldsymbol{y}} - \boldsymbol{y}\right\|_2^2$. Still, such bi-level optimizations are typically challenging to solve (Bard, 1991; 2013). Differentiating directly through the inner optimization $\operatorname{argmin}_{\boldsymbol{\theta}} \mathcal{L}(f(X_{\mathrm{dp}}; \boldsymbol{\theta}), \boldsymbol{y}_{\mathrm{dp}})$ with respect to the corrupted training data X_{p} is impractical for two reasons: (i) backpropagating through an iterative process incurs a significant performance penalty, even when using advanced checkpointing techniques (Walther & Griewank, 2004) and (ii) the gradients obtained by backpropagating through SGD are too noisy to be useful (Hospedales et al., 2020). To overcome these challenges, we propose to use a closed-form kernel to model the training dynamics of the neural network. This dramatically simplifies and stabilizes our loss, which becomes

$$\mathcal{L}_{\mathrm{backdoor}}(K_{\mathrm{dp,dpta}}, \boldsymbol{y}_{\mathrm{dpta}}) \;=\; \frac{1}{2}\left\|\boldsymbol{y}_{\mathrm{dp}}^{\top} K_{\mathrm{dp,dp}}^{-1} K_{\mathrm{dp,ta}} - \boldsymbol{y}_{\mathrm{ta}}\right\|_2^2, \tag{2}$$

where we plugged in the closed-form solution of the inner optimization from the *kernel linear regression model*, which we can easily differentiate with respect to $K_{\mathrm{dp,dpta}}$. We use $K : \mathcal{X} \times \mathcal{X} \to \mathbb{R}$ to denote a kernel function of choice, $K(X, X')$ to denote the $|X| \times |X'|$

kernel matrix with $K(X, X')_{i,j} = K(X_i, X'_j)$, and subscripts as shorthand for block matrices, e.g. $K_{\mathrm{a,dp}} = [K(X_{\mathrm{a}}, X_{\mathrm{d}}) \quad K(X_{\mathrm{a}}, X_{\mathrm{p}})]$. This simplification does not come for free, as kernel-designed poisons might not generalize to the neural network training that we desire to backdoor. Empirically demonstrating in §3 that there is little loss in transferring our attack to neural network is one of our main goals (see Table 2).

Greedy initialization. The optimization problem in Eq. (1) is nonconvex. Empirically, we find that the optimization always converges to a local minima that is close to the initialization of the poison images. We propose a greedy algorithm to select the initial set of images to start the optimization from. The algorithm proceeds by applying the trigger function $P(\cdot)$ to every image in the training set and, incrementally in a greedy fashion, selecting the image that has the greatest reduction in the backdoor loss when added to the poison set. This is motivated by our analysis in §4, which encourages poisons with small perturbation.

2.1 Ablation study

We perform an ablation study on the three components at the beginning of this section to demonstrate that they are all necessary. The alternatives are: ($\mathbf{1}'$) the empirical neural tangent kernel but with weights taken from random initialization of the model weights; ($\mathbf{1}''$) the infinite-width neural tangent kernel; (removing **2**) sampling the initial set of images from a standard Gaussian, (removing **3**) using the greedy initial poison set without any optimization. ASR for various combinations are shown in Table 1. The stark difference between our approach (**1**+**2**+**3**) and the rest suggests that all components are important in achieving a strong attack. Random initialization (**1**+**3**) fails as coupled examples that are very close to the clean image space but have different labels is critical in achieving strong attacks as shown in Fig. 3. Without our proposed optimization (**1**+**2**), the attack is weak. Attacks designed with different choices of neural tangent kernels ($\mathbf{1}'$+**2**+**3** and $\mathbf{1}''$+**2**+**3**) work well on the kernel models they were designed for, but the attack fails to transfer to the original neural network, suggesting that they are less accurate models of the network training.

Table 1: Ablation study under the setting of Fig. 1 with $m = 10$.

ablation	ASR
1 + **2** + **3**	72.1 %
1 + **3**	12.0 %
1 + **2**	16.2 %
$\mathbf{1}'$ + **2** + **3**	11.3 %
$\mathbf{1}''$ + **2** + **3**	23.1 %

3 Experimental results

We attack a WideResNet-34-5 Zagoruyko & Komodakis (2016) ($d \approx 10^7$) with GELU activations Hendrycks & Gimpel (2016) so that our network will satisfy the smoothness assumption in Appendix B.1.2. Additionally, we do not use batch normalization which is not yet supported by the neural tangent kernel library we use Novak et al. (2020). Our network is trained with SGD on a 2 label subset of CIFAR-10 Krizhevsky (2009). The particular pair of labels is "truck" and "deer" which was observed in Hayase et al. (2021) to be relatively difficult to backdoor since the two classes are easy to distinguish. We consider two backdoor triggers: the periodic image trigger of Barni et al. (2019) and a 3×3 checker patch applied at a random position in the image. These two triggers represent sparse control over images at test time in frequency and image space respectively. Results for the periodic trigger are given here while results for the patch trigger are given in Appendix C.1.

To fairly evaluate performance, we split the CIFAR-10 training set into an inner training set and validation set containing 80% and 20% of the images respectively. We run NTBA with the inner training set as D_{d}, the inner validation set as D_{t}, and the inner validation set with the trigger applied as D_{a}. Our neural network is then trained on $D_{\mathrm{d}} \cup D_{\mathrm{p}}$ and tested on the CIFAR-10 test set.

We also attack a pretrained ConvNeXt Liu et al. (2022) finetuned on a 2 label subset of ImageNet, following the setup of Saha et al. (2020) with details given in Appendix C.2. We describe the computational resources used to perform our attack in Appendix B.4.

3.1 NTBA makes backdoor attacks significantly more efficient

Our main results show that (*i*) as expected, there are some gaps in ASR when applying NTK-designed poison examples to neural network training, but (*ii*) NTK-designed poison examples still manage to be significantly stronger compared to sampling baseline. The most relevant metric is the test results of neural network training evaluated on the original validation set with the trigger applied, $\text{asr}_{\text{nn,te}}$. In Table 2, to achieve $\text{asr}_{\text{nn,te}} = 90.7\%$, NTBA requires 30 poisons, which is an order of magnitude fewer than the sampling baseline. The ASR for backdooring kernel regressions is almost perfect, as it is what NTBA is designed to do; we consistently get high $\text{asr}_{\text{ntk,te}}$ with only a few poisons. Perhaps surprisingly, we show that these NTBA-designed attacks can be used as is to attack regular neural network training and achieve ASR significantly higher than the commonly used baseline in Table 2, Figs. 1 and 9 to 11 for WideResNet trained on CIFAR-10 subtasks and ConvNeXt trained on ImageNet subtasks, NTBA tailored for patch and periodic triggers, respectively. ASR results are percentages and we omit % in this section.

Table 2: ASR results for NTK and NN ($\text{asr}_{\cdot,\text{ntk}}$ and $\text{asr}_{\cdot,\text{nn}}$) at train and test time ($\text{asr}_{\text{tr},\cdot}$ and $\text{asr}_{\text{te},\cdot}$). The NTBA attack transferred to neural networks is significantly stronger than the sampling based attack using the same periodic trigger across a range of poison budgets m. A graph version of this table is in Fig. 1.

	ours				sampling		sampling
m	$\text{asr}_{\text{ntk,tr}}$	$\text{asr}_{\text{ntk,te}}$	$\text{asr}_{\text{nn,tr}}$	$\text{asr}_{\text{nn,te}}$	$\text{asr}_{\text{nn,te}}$	m	$\text{asr}_{\text{nn,te}}$
1	100.0	85.2	0.2	11.0	5.9	0	5.5
3	100.0	92.8	5.6	35.2	7.6	100	79.1
10	100.0	95.2	65.2	72.1	21.3	300	89.3
30	100.0	96.4	94.2	90.7	49.6	1000	95.0

3.2 The attacker does not need to know all the training data

In our preceding experiments, the attacker has knowledge of the entire training set and a substantial quantity of validation data. In these experiments, the attacker is given a β fraction of the 2-label CIFAR-10 subset's train and validation sets. The backdoor is computed using only this partial data and the neural network is then run on the full data. NTBA degrades gracefully as the amount of information available to the attacker is reduced. Results for $m = 10$ are shown in Table 3.

Table 3: ASR decreases gracefully with the attacker knowing only β fraction of the data.

β	1.0	0.75	0.5	0.25
$\text{asr}_{\text{nn,te}}$	96.3	94.7	78.5	73.4

3.3 Is neural tangent kernel special?

Given the extreme vulnerability of NTKs (e.g., $\text{asr}_{\text{ntk,te}} = 85.2$ with one poison in Table 2), it is natural to ask if other kernel models can be similarly backdoored. To test this hypothesis, we apply the optimization from NTBA to both NTK and the standard Laplace kernel on the CIFAR-10 sub-task, starting from a random initialization. Although the Laplace kernel is given ten times more poison points, the optimization of NTBA can only achieve 11% ASR, even on the training data. In contrast, NTBA with the NTK yields a 100% train-ASR, with the clean accuracy for both kernels remaining the same. This suggests that Laplace kernel is not able to learn the poison without sacrificing the accuracy on clean data points. In §5, we further investigate what makes NTK (and hence neural networks) special.

Table 4: results for directly attacking the NTK and Laplace kernels on CIFAR-10 with a periodic trigger. acc_{tr} refers to clean accuracy after training on corrupted data.

m	kernel	acc_{tr}	asr_{tr}
1	NTK	93%	100%
10	Laplace	93%	11%

4 Interpreting the NTBA-designed poison examples

We show the images produced by NTBA in Fig. 3. Comparing second and third rows of Fig. 3, observe that the optimization generally reduces the magnitude of the trigger. Precise measurements in Figs. 4 and 5 further show that the magnitude of the train-time trigger learned via NTBA gets smaller as we decrease the number of injected poison examples m.

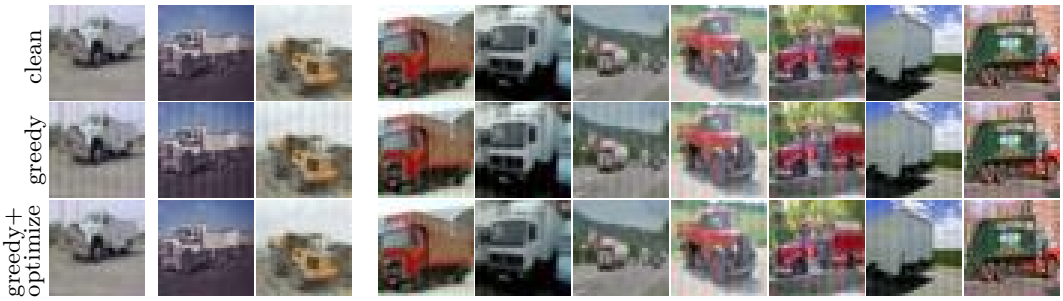

(a) $m = 1$ (b) $m = 3$ (c) $m = 10$

Figure 3: Images produced by NTBA for period trigger and $m \in \{1, 3, 10\}$. The top row shows the original clean image of the greedy initialization, the middle row shows the greedy initialization that includes the trigger, and the bottom row shows the final poison image after optimization. Duplicate images, for example the first poison image for $m = 3$, have been omitted to save space.

We analyze kernel linear regression to show that *backdoor attacks increase in strength as the poison images get closer to the manifold of clean data.* This provides an interpretation of the NTBA-designed poison examples. Given training data $D_{\mathrm{d}} = (X_{\mathrm{d}} \in \mathbb{R}^{n \times k}, \boldsymbol{y}_{\mathrm{d}} \in \{\pm 1\}^n)$ and a generic kernel K, the prediction of a kernel linear regression model trained on D_{d} and tested on some $\boldsymbol{x} \in \mathbb{R}^k$ is

$$f(\boldsymbol{x}; D_{\mathrm{d}}) \quad \triangleq \quad \boldsymbol{y}_{\mathrm{d}}^{\top} K(X_{\mathrm{d}}, X_{\mathrm{d}})^{-1} K(X_{\mathrm{d}}, \boldsymbol{x}), \tag{3}$$

where $K(\,\cdot\,,\,\cdot\,)$ denotes the kernel matrix over the data. For simplicity, suppose we are adding a single poison example $D_{\mathrm{p}} = \{(\boldsymbol{x}_{\mathrm{p}}, y_{\mathrm{p}})\}$ and testing on a single point $\boldsymbol{x}_{\mathrm{a}}$. For the attack to succeed, the injected poison example needs to change the prediction of $\boldsymbol{x}_{\mathrm{a}}$ by ensuring that

$$\underbrace{f(\boldsymbol{x}_{\mathrm{a}}; D_{\mathsf{d}} \cup \{(\boldsymbol{x}_{\mathrm{p}}, y_{\mathrm{p}})\})}_{\text{poisoned model prediction}} - \underbrace{f(\boldsymbol{x}_{\mathrm{a}}; D_{\mathsf{d}})}_{\text{clean model prediction}} = \frac{\phi(\boldsymbol{x}_{\mathrm{p}})(I - P)\phi(\boldsymbol{x}_{\mathrm{a}})^{\top}}{\phi(\boldsymbol{x}_{\mathrm{p}})(I - P)\phi(\boldsymbol{x}_{\mathrm{p}})^{\top}} (y_{\mathrm{p}} - f(\boldsymbol{x}_{\mathrm{p}}; D_{\mathsf{d}})) \tag{4}$$

is sufficiently large, where $\phi : \mathcal{X} \to \mathbb{R}^d$ is a feature map of kernel K such that $K(\boldsymbol{x}, \boldsymbol{y}) = \langle \phi(\boldsymbol{x}), \phi(\boldsymbol{y}) \rangle$, and $P = \Phi^{\top}(\Phi\Phi^{\top})^{-1}\Phi$ is the hat matrix of Φ (i.e. P projects onto the span of the rows of Φ) where Φ is the matrix with rows $\phi(\boldsymbol{x})$ for $\boldsymbol{x} \in X_{\mathrm{d}}$. Eq. (4) follows from the Schur complement after adding one row and column to the kernel matrix $K(X_{\mathrm{d}}, X_{\mathrm{d}})$ and adding one dimension to each of $\boldsymbol{y}_{\mathrm{d}}$ and $K(X_{\mathrm{d}}, \boldsymbol{x})$ in Eq. (3). We assume that both $\boldsymbol{x}_{\mathrm{p}}$ and $\boldsymbol{x}_{\mathrm{a}}$ are small perturbations of clean data points, and let $\boldsymbol{\Delta}_{\mathrm{p}} \triangleq \widetilde{\boldsymbol{x}}_{\mathrm{p}} - \boldsymbol{x}_{\mathrm{p}}$ and $\boldsymbol{\Delta}_{\mathrm{a}} \triangleq \widetilde{\boldsymbol{x}}_{\mathrm{a}} - \boldsymbol{x}_{\mathrm{a}}$ respectively denote the train-time perturbation and the test-time trigger for some clean data points $\widetilde{\boldsymbol{x}}_{\mathrm{p}}, \widetilde{\boldsymbol{x}}_{\mathrm{a}} \in X_{\mathrm{d}}$. In the naive periodic attack, both $\boldsymbol{\Delta}_{\mathrm{p}}$ and $\boldsymbol{\Delta}_{\mathrm{a}}$ are the periodic patterns we add. Our goal is to find out which choice of the train-time perturbation, $\boldsymbol{\Delta}_{\mathrm{p}}$, would make the attack stronger (for the given test-time trigger $\boldsymbol{\Delta}_{\mathrm{a}}$).

The powerful poison examples discovered via the proposed NTBA show the following patterns. In Fig. 4, each pixel shows the norm of the three channels of the perturbation $\boldsymbol{\Delta}_{\mathrm{p}}$ for a single poison example with the same closest clean image; the corresponding train examples are explicitly shown in Fig. 3a. The range of the pixel norm 0.2 is after data standardization normalized by the standard deviation for that pixel. In Figs. 4a to 4d, we see that the $\boldsymbol{\Delta}_{\mathrm{p}}$ aligns with the test-time trigger $\boldsymbol{\Delta}_{\mathrm{a}}$ in Fig. 4e, but with reduced amplitude and some fluctuations. When the allowed number of poisoned examples, m, is small, NTBA makes each poison example more powerful by reducing the magnitude of the perturbation $\boldsymbol{\Delta}_{\mathrm{p}}$. In Fig. 5,

the perturbations grow larger as we increase the number of poisoned examples constructed with our proposed attack NTBA. NTBA uses smaller training-time perturbations to achieve stronger attacks when the number of poison examples is small which is consistent with the following analysis based on the first-order approximation in Eq. (5).

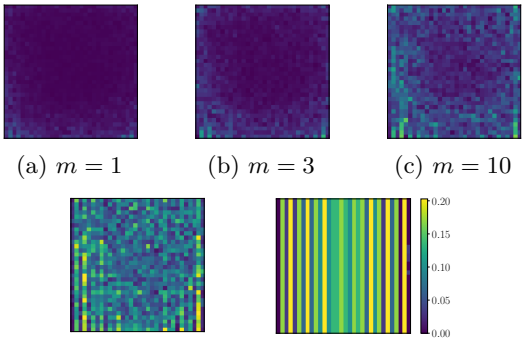

(a) $m = 1$ (b) $m = 3$ (c) $m = 10$

(d) $m = 30$ (e) test $\boldsymbol{\Delta}_{\mathrm{a}}$

Figure 4: As the number of poison examples, m, decrease, NTBA makes each poison example stronger by reducing the magnitude of the pixels of the train-time perturbation $\boldsymbol{\Delta}_{\mathrm{p}}$.

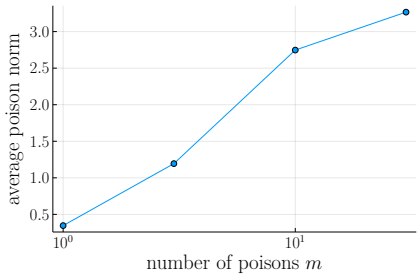

Figure 5: The average norm difference, $\|\boldsymbol{\Delta}_{\mathrm{p}}\|$, between each poison image automatically discovered by NTBA and the closest clean image, after running NTBA with different choices of m.

To explain this phenomenon, we take Taylor approximations of ϕ at $\widetilde{\boldsymbol{x}}_{\mathrm{p}}$ and $\widetilde{\boldsymbol{x}}_{\mathrm{a}}$ and obtain,

$$\begin{aligned} & f(\boldsymbol{x}_{\mathrm{a}}; D_{\mathsf{d}} \cup \{(\boldsymbol{x}_{\mathrm{p}}, y_{\mathrm{p}})\}) - f(\boldsymbol{x}_{\mathrm{a}}; D_{\mathsf{d}}) \\ & \approx \frac{(\phi(\widetilde{\boldsymbol{x}}_{\mathrm{p}}) + \mathrm{D}\phi(\widetilde{\boldsymbol{x}}_{\mathrm{p}})\boldsymbol{\Delta}_{\mathrm{p}})(I-P)(\phi(\widetilde{\boldsymbol{x}}_{\mathrm{a}}) + \mathrm{D}\phi(\widetilde{\boldsymbol{x}}_{\mathrm{a}})\boldsymbol{\Delta}_{\mathrm{a}})^{\top}}{(\phi(\widetilde{\boldsymbol{x}}_{\mathrm{p}}) + \mathrm{D}\phi(\widetilde{\boldsymbol{x}}_{\mathrm{p}})\boldsymbol{\Delta}_{\mathrm{p}})(I-P)(\phi(\widetilde{\boldsymbol{x}}_{\mathrm{p}}) + \mathrm{D}\phi(\widetilde{\boldsymbol{x}}_{\mathrm{p}})\boldsymbol{\Delta}_{\mathrm{p}})^{\top}} (y_{\mathrm{p}} - f(\boldsymbol{x}_{\mathrm{p}}; D_{\mathsf{d}})) \\ & = \underbrace{\frac{\langle \mathrm{D}\phi(\widetilde{\boldsymbol{x}}_{\mathrm{p}})\boldsymbol{\Delta}_{\mathrm{p}}, \mathrm{D}\phi(\widetilde{\boldsymbol{x}}_{\mathrm{a}})\boldsymbol{\Delta}_{\mathrm{a}}\rangle_{(I-P)}}{\|\mathrm{D}\phi(\widetilde{\boldsymbol{x}}_{\mathrm{p}})\boldsymbol{\Delta}_{\mathrm{p}}\|^2_{(I-P)}}}_{\triangleq A} \underbrace{(y_{\mathrm{p}} - f(\boldsymbol{x}_{\mathrm{p}}; D_{\mathsf{d}}))}_{\approx 2}, \end{aligned}$$

where $\mathrm{D}\phi(\widetilde{\boldsymbol{x}})$ denotes the Jacobian of the feature mapping ϕ at $\widetilde{\boldsymbol{x}}$ and w.l.o.g. we assume that $y_{\mathrm{p}} = 1$ and $f(\boldsymbol{x}_{\mathrm{p}}; D_{\mathsf{d}}) \approx -1$. The last step follows because $(I-P)\phi(\widetilde{\boldsymbol{x}}_{\mathrm{a}}) = (I-P)\phi(\widetilde{\boldsymbol{x}}_{\mathrm{p}}) = \mathbf{0}$. Note that if $A = 1$, then $f(\boldsymbol{x}_{\mathrm{a}}; D_{\mathsf{d}} \cup \{(\boldsymbol{x}_{\mathrm{p}}, y_{\mathrm{p}})\}) = y_{\mathrm{p}}$ which would imply a succesful attack for $\boldsymbol{x}_{\mathrm{a}}$. Since the goal of the attack is to control the prediction whenever $\boldsymbol{\Delta}_{\mathrm{a}}$ is applied to *any* clean point $\widetilde{\boldsymbol{x}}$, there may exist some $\widetilde{\boldsymbol{x}}$ where $\mathrm{D}\phi(\widetilde{\boldsymbol{x}}_{\mathrm{a}})\boldsymbol{\Delta}_{\mathrm{a}}$ does not align well with $\mathrm{D}\phi(\widetilde{\boldsymbol{x}}_{\mathrm{p}})\boldsymbol{\Delta}_{\mathrm{p}}$, which would make the numerator of A small. For the backdoor to succeed for these points, $\|\mathrm{D}\phi(\widetilde{\boldsymbol{x}}_{\mathrm{p}})\boldsymbol{\Delta}_{\mathrm{p}}\|_{(I-P)}$ must be small enough to overcome this misalignment, since the denominator of A scales as $\|\mathrm{D}\phi(\widetilde{\boldsymbol{x}}_{\mathrm{p}})\boldsymbol{\Delta}_{\mathrm{p}}\|^2_{(I-P)}$ while the numerator scales as $\|\mathrm{D}\phi(\widetilde{\boldsymbol{x}}_{\mathrm{p}})\boldsymbol{\Delta}_{\mathrm{p}}\|_{(I-P)}$. In particular, for the attack to succeed on a set of poisoned data points X_{a}, we need

$$\|\mathrm{D}\phi(\widetilde{\boldsymbol{x}}_{\mathrm{p}})\boldsymbol{\Delta}_{\mathrm{p}}\|_{(I-P)} \leq c \left(\min_{\boldsymbol{x}_{\mathrm{a}} \in X_{\mathrm{a}}} \left\langle \frac{\mathrm{D}\phi(\widetilde{\boldsymbol{x}}_{\mathrm{p}})\boldsymbol{\Delta}_{\mathrm{p}}}{\|\mathrm{D}\phi(\widetilde{\boldsymbol{x}}_{\mathrm{p}})\boldsymbol{\Delta}_{\mathrm{p}}\|_{(I-P)}}, \mathrm{D}\phi(\widetilde{\boldsymbol{x}}_{\mathrm{a}})\boldsymbol{\Delta}_{\mathrm{a}} \right\rangle_{(I-P)} \right), \tag{5}$$

for some constant $c > 0$. Note that the test-time trigger $\boldsymbol{\Delta}_{\mathrm{a}}$ and therefore the distribution of $\boldsymbol{x}_{\mathrm{a}}$'s is fixed. Therefore Eq. (5) can be satisfied by choosing the train-time perturbation $\boldsymbol{\Delta}_{\mathrm{p}}$ to have small enough norm on the LHS of Eq. (5). This implies that smaller perturbations in the train-time poison data are able to successfully change the predictions on more examples at test-time, and hence they correspond to a stronger attack. We can make this connection more realistic by considering multiple poisoned examples injected together. As the size $m \triangleq |D_{\mathrm{p}}|$ of the injected poisoned dataset D_{p} increases, we may distribute the poisoned examples so that each test point $\boldsymbol{x}_{\mathrm{a}}$ is covered by some poison point $\boldsymbol{x}_{\mathrm{p}} \in X_{\mathrm{p}}$ that aligns well with it. Since the worst-case alignment between poison and test data will be higher, the RHS of Eq. (5) will be larger so the LHS may be larger as well. This means that for

each poison, the size of the trigger $\|\mathrm{D}\phi(\widetilde{\boldsymbol{x}}_{\mathrm{p}})\boldsymbol{\Delta}_{\mathrm{p}}\|_{(I-P)}$ may be larger (and still achieve a high attack success rate) when we are adding more poison data.

Two further insights from Eq. (5) shows the strengths of NTBA. First, Eq. (5) suggests that there is potential for improvement by designing train-time perturbations $\boldsymbol{\Delta}_{\mathrm{p}}$ that adapt to the local geometry of the feature map, represented by $\mathrm{D}\phi(\widetilde{\boldsymbol{x}}_{\mathrm{p}}), \mathrm{D}\phi(\widetilde{\boldsymbol{x}}_{\mathrm{a}})$, around clean data points $\widetilde{\boldsymbol{x}}_{\mathrm{p}}, \widetilde{\boldsymbol{x}}_{\mathrm{a}}$. We propose using a data-driven optimization to automatically discover such strong perturbations. Second, our analysis suggests that we need the knowledge of the manifold of clean data to design strong poisoned images that are close to the manifold. Since the manifold is challenging to learn from data, we explicitly initialize the optimization near carefully selected clean images $\widetilde{\boldsymbol{x}}_{\mathrm{p}}$, allowing the optimization to easily control the size of the difference $\boldsymbol{\Delta}_{\mathrm{p}}$. We show in our ablation study in §2.1 that both components are critical for designing strong attacks.

5 Why are NNs so vulnerable to backdoor attacks?

NTBA showcases the vulnerability of DNNs to backdoor attacks. We investigate the cause of such vulnerability by comparing the infinite-width NTK with the standard Laplace kernel.

NTK gives more influence to far away data points. The Laplace kernel gives more influence to points that are closer. For example, Laplace-kernel linear regression converges to a 1-nearest neighbor predictor in the limit as the bandwidth $\sigma \to 0$, which is naturally robust against few-shot backdoor attacks. In contrast, we conjecture that the NTK (and hence neural network) gives *more* influence to points as they become more distant. We confirm this by visualizing the two kernels with matched bandwidths in the normal and tangent direction to a unit sphere. For details, we refer to Appendix D.

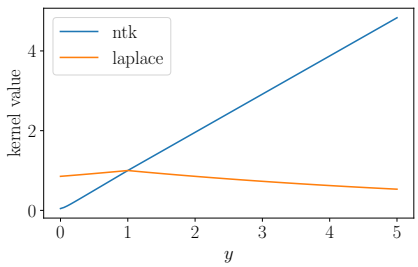

(a) Kernel behavior *normal* to unit sphere. The plot shows $K(\boldsymbol{e}_1, y\boldsymbol{e}_1)$ for both the NTK and Laplace kernels where $\boldsymbol{e}_1$ is a unit vector. Note that the NTK increases with y, while the Laplace kernel peaks at $y = 1$.

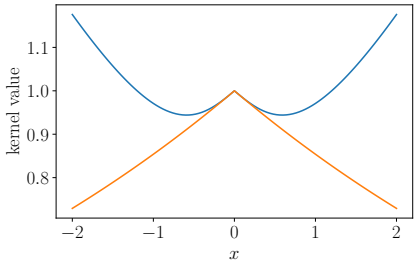

(b) Kernel behavior *tangent* to unit sphere. The plot shows $K(\boldsymbol{e}_1, \boldsymbol{e}_1 + x\boldsymbol{e}_2)$ for both the NTK and Laplace kernels where $\boldsymbol{e}_1, \boldsymbol{e}_2$ are orthogonal unit vectors. The two kernel behave similarly near $x = 0$ but diverge rapidly away from 0.

Figure 6: Kernel behavior off the unit sphere shows that the NTK approaches oblique asymptotes as either $|x|$ or y, increases, while the Laplace kernel decreases in the same limit.

NTK is more vulnerable to few-shot backdoor attacks. We demonstrate with a toy example that NTK is more influenced by far away points, which causes it to be more vulnerable to some few-shot backdoor attacks. We use a synthetic backdoor dataset in 3 dimensions (x, y, z) consisting of clean data $([\widetilde{x} \quad 1 \quad 0]^\top, 1)$ and $([\widetilde{x} \quad -1 \quad 0]^\top, -1)$ for $\widetilde{x} \in \{-100, -99, \ldots, 100\}$. Here, the x dimension represents the diversity of the dataset, the y dimension represents the true separation between the two classes, and the z dimension is used to trigger the backdoor attack. We choose test-time trigger $P(\boldsymbol{v}) = \boldsymbol{v} + [0 \quad 0 \quad 1]^\top$ for a clean negative labelled point $\boldsymbol{v}$ and add a single train-time poison data point $(0, -1, \widetilde{z})$. For the Laplace kernel, we compute the best choice of $\widetilde{z}$ which is $\widetilde{z} = 1$. For the NTK, the backdoor increases in strength as $\widetilde{z} \to 0^+$ (we chose $\widetilde{z} = 1 \times 10^{-6}$).

In Fig. 7d we see that the backdoor is not successful for the Laplace kernel, only managing to flip the prediction of a single backdoor test point. This is because the influence of the poison point rapidly drops off as $|x|$ increases. For $|x| > 10$ the poison has a negligible effect

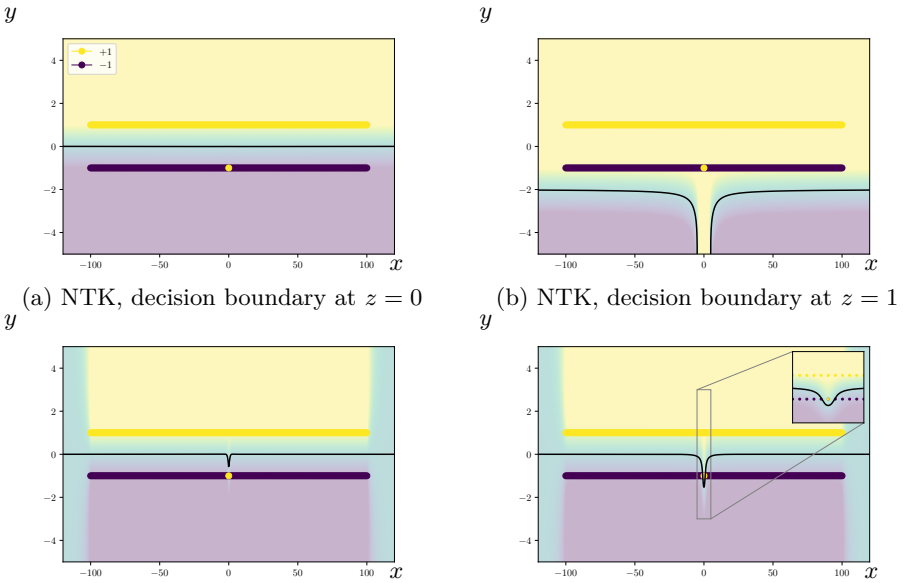

(a) NTK, decision boundary at $z = 0$ (b) NTK, decision boundary at $z = 1$

(c) Laplace, decision boundary at $z = 0$ (d) Laplace, decision boundary at $z = 1$

Figure 7: The decision boundaries at $z = 0$ (black solid line) and corresponding predictions (background shading) on the $z = 0$ plane are similar for NTK and Laplace kernel, explaining the similar clean accuracy in Table 4. The decision boundary at $z = 1$ shows that the trigger fails to generalize to test examples for Laplace kernel. All points in the training dataset are shown regardless of their z-coordinate. Note that the solid bars are actually discrete points with overlapping markers and the yellow point at $(0, -1)$ is the single poison point.

on the predictions of the model. In contrast, we see in Fig. 7b that the NTK was successfully backdoored and the predictions of all test points can be flipped by the trigger $P(\cdot)$. This is due to the influence of the poison point remains high even from a great distance.

6 Conclusion

We study the fundamental trade-off in backdoor attacks between the number of poisoned examples that need to be injected and the resulting attack success rate and bring a new perspective on backdoor attacks, borrowing tools from kernel methods. Through an ablation study in Table 1, we demonstrate that every component in the Neural Tangent Backdoor Attack (NTBA) is necessary in finding train-time poison examples that are significantly more powerful. We experiment on CIFAR and ImageNet subsets with WideResNet-34-5 and ConvNeXt architectures for periodic triggers and patch triggers, and show that, in some cases, NTBA requires an order of magnitude smaller number of poison examples to reach a target attack success rate compare to the baseline.

Next, we borrow the analysis of kernel linear regression to provide an interpretation of the NTBA-designed poison examples. The strength of the attack increases as we decrease the magnitude of the trigger used in the poison training example, especially when it is coupled with a clean data that is close in the image space. Finally, we compare neural tangent kernel and the Laplace kernel to investigate why the NTK is so vulnerable to backdoor attacks. Although this attack may be used for harmful purposes, our goal is to show the existence of strong backdoor attacks to motivate continued research into backdoor defenses and inspire practitioners to carefully secure their machine learning pipelines. The main limitation of our approach is a lack of scalability, as the cost of computing the NTK predictions Eq. (2) scales cubically in the number of datapoints. In the future, we plan to apply techniques for scaling the NTK Meanti et al. (2020); Rudi et al. (2017); Zandieh et al. (2021) to our attack.

References

Hojjat Aghakhani, Dongyu Meng, Yu-Xiang Wang, Christopher Kruegel, and Giovanni Vigna. Bullseye polytope: A scalable clean-label poisoning attack with improved transferability. In *2021 IEEE European Symposium on Security and Privacy (EuroS&P)*, pp. 159–178. IEEE, 2021.

Sina Alemohammad, Zichao Wang, Randall Balestriero, and Richard Baraniuk. The recurrent neural tangent kernel. In *International Conference on Learning Representations*, 2020.

Dan Alistarh, Zeyuan Allen-Zhu, and Jerry Li. Byzantine stochastic gradient descent. In *Advances in Neural Information Processing Systems*, pp. 4613–4623, 2018.

Sanjeev Arora, Simon S Du, Zhiyuan Li, Ruslan Salakhutdinov, Ruosong Wang, and Dingli Yu. Harnessing the power of infinitely wide deep nets on small-data tasks. In *International Conference on Learning Representations*, 2019.

Eugene Bagdasaryan, Andreas Veit, Yiqing Hua, Deborah Estrin, and Vitaly Shmatikov. How to backdoor federated learning. In *International Conference on Artificial Intelligence and Statistics*, pp. 2938–2948. PMLR, 2020.

Jonathan F Bard. Some properties of the bilevel programming problem. *Journal of optimization theory and applications*, 68(2):371–378, 1991.

Jonathan F Bard. *Practical bilevel optimization: algorithms and applications*, volume 30. Springer Science & Business Media, 2013.

Mauro Barni, Kassem Kallas, and Benedetta Tondi. A new backdoor attack in cnns by training set corruption without label poisoning. In *2019 IEEE International Conference on Image Processing (ICIP)*, pp. 101–105. IEEE, 2019.

Peva Blanchard, Rachid Guerraoui, and Julien Stainer. Machine learning with adversaries: Byzantine tolerant gradient descent. In *Advances in Neural Information Processing Systems*, pp. 119–129, 2017.

Zalán Borsos, Mojmir Mutny, and Andreas Krause. Coresets via bilevel optimization for continual learning and streaming. *Advances in Neural Information Processing Systems*, 33: 14879–14890, 2020.

James Bradbury, Roy Frostig, Peter Hawkins, Matthew James Johnson, Chris Leary, Dougal Maclaurin, George Necula, Adam Paszke, Jake VanderPlas, Skye Wanderman-Milne, and Qiao Zhang. JAX: composable transformations of Python+NumPy programs, 2018. URL `http://github.com/google/jax`.

Lin Chen and Sheng Xu. Deep neural tangent kernel and laplace kernel have the same RKHS. In *International Conference on Learning Representations*, 2021. URL `https://openreview.net/forum?id=vK9WrZ0QYQ`.

Lingjiao Chen, Hongyi Wang, Zachary Charles, and Dimitris Papailiopoulos. Draco: Byzantine-resilient distributed training via redundant gradients. In *International Conference on Machine Learning*, pp. 903–912. PMLR, 2018.

Xinyun Chen, Chang Liu, Bo Li, Kimberly Lu, and Dawn Song. Targeted backdoor attacks on deep learning systems using data poisoning. *arXiv preprint arXiv:1712.05526*, 2017.

Edward Chou, Florian Tramer, and Giancarlo Pellegrino. Sentinet: Detecting localized universal attacks against deep learning systems. In *2020 IEEE Security and Privacy Workshops (SPW)*, pp. 48–54. IEEE, 2020.

Khoa Doan, Yingjie Lao, and Ping Li. Backdoor attack with imperceptible input and latent modification. *Advances in Neural Information Processing Systems*, 34, 2021a.

Khoa Doan, Yingjie Lao, Weijie Zhao, and Ping Li. Lira: Learnable, imperceptible and robust backdoor attacks. In *Proceedings of the IEEE/CVF International Conference on Computer Vision*, pp. 11966–11976, 2021b.

Simon Du, Jason Lee, Haochuan Li, Liwei Wang, and Xiyu Zhai. Gradient descent finds global minima of deep neural networks. In *International conference on machine learning*, pp. 1675–1685. PMLR, 2019a.

Simon S Du, Xiyu Zhai, Barnabas Poczos, and Aarti Singh. Gradient descent provably optimizes over-parameterized neural networks. In *International Conference on Learning Representations*, 2018.

Simon S Du, Kangcheng Hou, Russ R Salakhutdinov, Barnabas Poczos, Ruosong Wang, and Keyulu Xu. Graph neural tangent kernel: Fusing graph neural networks with graph kernels. *Advances in neural information processing systems*, 32, 2019b.

Stanislav Fort, Gintare Karolina Dziugaite, Mansheej Paul, Sepideh Kharaghani, Daniel M Roy, and Surya Ganguli. Deep learning versus kernel learning: an empirical study of loss landscape geometry and the time evolution of the neural tangent kernel. *Advances in Neural Information Processing Systems*, 33:5850–5861, 2020.

Yansong Gao, Change Xu, Derui Wang, Shiping Chen, Damith C Ranasinghe, and Surya Nepal. Strip: A defence against trojan attacks on deep neural networks. In *Proceedings of the 35th Annual Computer Security Applications Conference*, pp. 113–125, 2019.

Amnon Geifman, Abhay Yadav, Yoni Kasten, Meirav Galun, David Jacobs, and Basri Ronen. On the similarity between the laplace and neural tangent kernels. *Advances in Neural Information Processing Systems*, 33:1451–1461, 2020.

Shafi Goldwasser, Michael P Kim, Vinod Vaikuntanathan, and Or Zamir. Planting undetectable backdoors in machine learning models. *arXiv preprint arXiv:2204.06974*, 2022.

Tianyu Gu, Brendan Dolan-Gavitt, and Siddharth Garg. Badnets: Identifying vulnerabilities in the machine learning model supply chain. *arXiv preprint arXiv:1708.06733*, 2017.

Junfeng Guo and Cong Liu. Practical poisoning attacks on neural networks. In *European Conference on Computer Vision*, pp. 142–158. Springer, 2020.

Jonathan Hayase, Weihao Kong, Raghav Somani, and Sewoong Oh. SPECTRE: Defending against backdoor attacks using robust statistics. In *International Conference on Machine Learning*, pp. 4129–4139. PMLR, 2021.

Dan Hendrycks and Kevin Gimpel. Gaussian error linear units (GELUs). *arXiv preprint arXiv:1606.08415*, 2016.

Timothy Hospedales, Antreas Antoniou, Paul Micaelli, and Amos Storkey. Meta-learning in neural networks: A survey. *arXiv preprint arXiv:2004.05439*, 2020.

Arthur Jacot, Franck Gabriel, and Clément Hongler. Neural tangent kernel: Convergence and generalization in neural networks. *Advances in neural information processing systems*, 31, 2018.

Peter Kairouz, H Brendan McMahan, Brendan Avent, Aurélien Bellet, Mehdi Bennis, Arjun Nitin Bhagoji, Keith Bonawitz, Zachary Charles, Graham Cormode, Rachel Cummings, et al. Advances and open problems in federated learning. *arXiv preprint arXiv:1912.04977*, 2019.

Diederick P Kingma and Jimmy Ba. Adam: A method for stochastic optimization. In *International Conference on Learning Representations (ICLR)*, 2015.

Pang Wei Koh, Jacob Steinhardt, and Percy Liang. Stronger data poisoning attacks break data sanitization defenses. *Machine Learning*, 111(1):1–47, 2022.

Soheil Kolouri, Aniruddha Saha, Hamed Pirsiavash, and Heiko Hoffmann. Universal litmus patterns: Revealing backdoor attacks in cnns. In *Proceedings of the IEEE/CVF Conference on Computer Vision and Pattern Recognition*, pp. 301–310, 2020.

Alex Krizhevsky. Learning multiple layers of features from tiny images. Technical report, 2009.

Jaehoon Lee, Samuel Schoenholz, Jeffrey Pennington, Ben Adlam, Lechao Xiao, Roman Novak, and Jascha Sohl-Dickstein. Finite versus infinite neural networks: an empirical study. *Advances in Neural Information Processing Systems*, 33:15156–15172, 2020.

Kimin Lee, Kibok Lee, Honglak Lee, and Jinwoo Shin. A simple unified framework for detecting out-of-distribution samples and adversarial attacks. In *Advances in Neural Information Processing Systems*, pp. 7167–7177, 2018.

Shaofeng Li, Minhui Xue, Benjamin Zi Hao Zhao, Haojin Zhu, and Xinpeng Zhang. Invisible backdoor attacks on deep neural networks via steganography and regularization. *IEEE Transactions on Dependable and Secure Computing*, 18(5):2088–2105, 2020.

Zhiyuan Li, Ruosong Wang, Dingli Yu, Simon S Du, Wei Hu, Ruslan Salakhutdinov, and Sanjeev Arora. Enhanced convolutional neural tangent kernels. *arXiv preprint arXiv:1911.00809*, 2019.

Shiyu Liang, Yixuan Li, and R Srikant. Enhancing the reliability of out-of-distribution image detection in neural networks. In *6th International Conference on Learning Representations, ICLR 2018*, 2018.

Kang Liu, Brendan Dolan-Gavitt, and Siddharth Garg. Fine-pruning: Defending against backdooring attacks on deep neural networks. In *International Symposium on Research in Attacks, Intrusions, and Defenses*, pp. 273–294. Springer, 2018.

Yunfei Liu, Xingjun Ma, James Bailey, and Feng Lu. Reflection backdoor: A natural backdoor attack on deep neural networks. In *European Conference on Computer Vision*, pp. 182–199. Springer, 2020.

Zhuang Liu, Hanzi Mao, Chao-Yuan Wu, Christoph Feichtenhofer, Trevor Darrell, and Saining Xie. A convnet for the 2020s. *arXiv preprint arXiv:2201.03545*, 2022.

Philip M Long. Properties of the after kernel. *arXiv preprint arXiv:2105.10585*, 2021.

Giacomo Meanti, Luigi Carratino, Lorenzo Rosasco, and Alessandro Rudi. Kernel methods through the roof: handling billions of points efficiently. *Advances in Neural Information Processing Systems*, 33:14410–14422, 2020.

Luis Muñoz-González, Battista Biggio, Ambra Demontis, Andrea Paudice, Vasin Wongrassamee, Emil C Lupu, and Fabio Roli. Towards poisoning of deep learning algorithms with back-gradient optimization. In *Proceedings of the 10th ACM workshop on artificial intelligence and security*, pp. 27–38, 2017.

Timothy Nguyen, Zhourong Chen, and Jaehoon Lee. Dataset meta-learning from kernel ridge-regression. In *International Conference on Learning Representations*, 2020.

Timothy Nguyen, Roman Novak, Lechao Xiao, and Jaehoon Lee. Dataset distillation with infinitely wide convolutional networks. *Advances in Neural Information Processing Systems*, 34, 2021.

Tuan Anh Nguyen and Anh Tuan Tran. Wanet-imperceptible warping-based backdoor attack. In *International Conference on Learning Representations*, 2020.

Roman Novak, Lechao Xiao, Jiri Hron, Jaehoon Lee, Alexander A. Alemi, Jascha Sohl-Dickstein, and Samuel S. Schoenholz. Neural tangents: Fast and easy infinite neural networks in python. In *International Conference on Learning Representations*, 2020. URL `https://github.com/google/neural-tangents`.

Roman Novak, Jascha Sohl-Dickstein, and Samuel Stern Schoenholz. Fast finite width neural tangent kernel. In *Fourth Symposium on Advances in Approximate Bayesian Inference*, 2021.

Krishna Pillutla, Sham M Kakade, and Zaid Harchaoui. Robust aggregation for federated learning. *arXiv preprint arXiv:1912.13445*, 2019.

Ambrish Rawat, Killian Levacher, and Mathieu Sinn. The devil is in the gan: Defending deep generative models against backdoor attacks. *arXiv preprint arXiv:2108.01644*, 2021.

Alessandro Rudi, Luigi Carratino, and Lorenzo Rosasco. Falkon: An optimal large scale kernel method. *Advances in neural information processing systems*, 30, 2017.

Aniruddha Saha, Akshayvarun Subramanya, and Hamed Pirsiavash. Hidden trigger backdoor attacks. In *Proceedings of the AAAI conference on artificial intelligence*, volume 34, pp. 11957–11965, 2020.

Ahmed Salem, Yannick Sautter, Michael Backes, Mathias Humbert, and Yang Zhang. Baaan: Backdoor attacks against autoencoder and gan-based machine learning models. *arXiv preprint arXiv:2010.03007*, 2020.

Mariia Seleznova and Gitta Kutyniok. Analyzing finite neural networks: Can we trust neural tangent kernel theory? In *Mathematical and Scientific Machine Learning*, pp. 868–895. PMLR, 2022.

Ali Shafahi, W Ronny Huang, Mahyar Najibi, Octavian Suciu, Christoph Studer, Tudor Dumitras, and Tom Goldstein. Poison frogs! targeted clean-label poisoning attacks on neural networks. *Advances in neural information processing systems*, 31, 2018.

Reza Shokri et al. Bypassing backdoor detection algorithms in deep learning. In *2020 IEEE European Symposium on Security and Privacy (EuroS&P)*, pp. 175–183. IEEE, 2020.

Jacob Steinhardt, Pang Wei W Koh, and Percy S Liang. Certified defenses for data poisoning attacks. In *Advances in neural information processing systems*, pp. 3517–3529, 2017.

Ziteng Sun, Peter Kairouz, Ananda Theertha Suresh, and H Brendan McMahan. Can you really backdoor federated learning? *arXiv preprint arXiv:1911.07963*, 2019.

Brandon Tran, Jerry Li, and Aleksander Madry. Spectral signatures in backdoor attacks. *Advances in neural information processing systems*, 31, 2018.

Alexander Turner, Dimitris Tsipras, and Aleksander Madry. Label-consistent backdoor attacks. *arXiv preprint arXiv:1912.02771*, 2019.

Pauli Virtanen, Ralf Gommers, Travis E. Oliphant, Matt Haberland, Tyler Reddy, David Cournapeau, Evgeni Burovski, Pearu Peterson, Warren Weckesser, Jonathan Bright, Stéfan J. van der Walt, Matthew Brett, Joshua Wilson, K. Jarrod Millman, Nikolay Mayorov, Andrew R. J. Nelson, Eric Jones, Robert Kern, Eric Larson, C J Carey, İlhan Polat, Yu Feng, Eric W. Moore, Jake VanderPlas, Denis Laxalde, Josef Perktold, Robert Cimrman, Ian Henriksen, E. A. Quintero, Charles R. Harris, Anne M. Archibald, Antônio H. Ribeiro, Fabian Pedregosa, Paul van Mulbregt, and SciPy 1.0 Contributors. SciPy 1.0: Fundamental Algorithms for Scientific Computing in Python. *Nature Methods*, 17:261–272, 2020. doi: 10.1038/s41592-019-0686-2.

Andrea Walther and Andreas Griewank. Advantages of binomial checkpointing for memory-reduced adjoint calculations. In *Numerical mathematics and advanced applications*, pp. 834–843. Springer, 2004.

Binghui Wang, Xiaoyu Cao, Neil Zhenqiang Gong, et al. On certifying robustness against backdoor attacks via randomized smoothing. *arXiv preprint arXiv:2002.11750*, 2020a.

Bolun Wang, Yuanshun Yao, Shawn Shan, Huiying Li, Bimal Viswanath, Haitao Zheng, and Ben Y Zhao. Neural cleanse: Identifying and mitigating backdoor attacks in neural networks. In *2019 IEEE Symposium on Security and Privacy (SP)*, pp. 707–723. IEEE, 2019.

Hongyi Wang, Kartik Sreenivasan, Shashank Rajput, Harit Vishwakarma, Saurabh Agarwal, Jy-yong Sohn, Kangwook Lee, and Dimitris Papailiopoulos. Attack of the tails: Yes, you really can backdoor federated learning. *Advances in Neural Information Processing Systems*, 33, 2020b.

Maurice Weber, Xiaojun Xu, Bojan Karlaš, Ce Zhang, and Bo Li. Rab: Provable robustness against backdoor attacks. *arXiv preprint arXiv:2003.08904*, 2020.

Pengfei Xia, Hongjing Niu, Ziqiang Li, and Bin Li. Enhancing backdoor attacks with multi-level mmd regularization. *IEEE Transactions on Dependable and Secure Computing*, 2022.

Chaofei Yang, Qing Wu, Hai Li, and Yiran Chen. Generative poisoning attack method against neural networks. *arXiv preprint arXiv:1703.01340*, 2017.

Greg Yang. Tensor programs ii: Neural tangent kernel for any architecture. *arXiv preprint arXiv:2006.14548*, 2020.

Yuanshun Yao, Huiying Li, Haitao Zheng, and Ben Y Zhao. Latent backdoor attacks on deep neural networks. In *Proceedings of the 2019 ACM SIGSAC Conference on Computer and Communications Security*, pp. 2041–2055, 2019.

Chia-Hung Yuan and Shan-Hung Wu. Neural tangent generalization attacks. In *International Conference on Machine Learning*, pp. 12230–12240. PMLR, 2021.

Sergey Zagoruyko and Nikos Komodakis. Wide residual networks. In *British Machine Vision Conference 2016*. British Machine Vision Association, 2016.

Amir Zandieh, Insu Han, Haim Avron, Neta Shoham, Chaewon Kim, and Jinwoo Shin. Scaling neural tangent kernels via sketching and random features. *Advances in Neural Information Processing Systems*, 34, 2021.

Shihao Zhao, Xingjun Ma, Xiang Zheng, James Bailey, Jingjing Chen, and Yu-Gang Jiang. Clean-label backdoor attacks on video recognition models. In *Proceedings of the IEEE/CVF Conference on Computer Vision and Pattern Recognition*, pp. 14443–14452, 2020.

Yufan Zhou, Zhenyi Wang, Jiayi Xian, Changyou Chen, and Jinhui Xu. Meta-learning with neural tangent kernels. *arXiv preprint arXiv:2102.03909*, 2021.